FUDMA Journal of Sciences (FJS)
ISSN online: 2616-1370
ISSN print: 2645 - 2944
Vol. 10 No. 6, March, 2026, pp 209 – 221
DOI: https://doi.org/10.33003/fjs-2026-1006-4897

OPTIMIZATION AND SIMULATIONS OF POWER SYSTEM STABILITY FACTS CONTROLLERS COORDINATED WITH POWER SYSTEM STABILIZER BASED-TIME DELAY

Johnson O. Aibangbee

Department of Electrical & Electronic Engineering, Benson Idahosa University, Benin City. Edo State, Nigeria.

*Corresponding authors' email: engr.aibangbee@gmail.com

ABSTRACT

Transmission time-delays in electrical power grid significantly causes adverse effect on performance of control systems and can lead to system failure. The study analyzes the simultaneous tuning of the power system stabilizer (PSS) and power system stability FACTS controller coordinated static synchronous series compensator (SSSC). The proposes controller was designed and optimized using combine grasshopper optimization algorithm (GOA) with fuzzy proportional-integral-derivative (F-PID) controllers to effectively fine-tuned control parameters to minimize the impact of time delay signals. Simulation conducted using MATLAB R2016a environment with simultaneous calculation of the objective functions. Results obtained from proposes GOA optimized controller with different loading conditions, disturbances and variations in signal transmission delays were compared with those of differential evolution (DE), genetic algorithm (GA) and Whale optimization algorithm (WOA). Results proved that in single machine infinite bus (SMIB) system, GOA provides superior damping oscillations, reduced peak deviation, reaches steady state faster and provide lowest values in terms of integral of time-weighted absolute error (ITAE), lower percentage overshoot, and faster settling times of 0.00206, -0.00061, and 2.65 seconds, compared to DE, GA and WOA of 0.00337, -0.00219 , 4.00 sec; 0.00318, -0.00223, 3.35 sec; and 0.002905, -0.00105, and 3.34 sec. whereas, for multi-machine system, the ITAE values with GOA is 0.0001806 compared to DE, GA, and WOA of 0.0002084, 0.0002007, and 0.0001832. The proposed GOA optimized controller reduced the objective function values by 16.29% better than WOA (14.53%), GA (14.53%), and DE (13.69%), in the SMIB system and 1.43%, 9.95%, and 13.33%, for the multi-machine systems.

Keywords: Damping Oscillations, Fuzzy Logic Controller, Grasshopper Optimization Algorithm, Integral Of Time-Weighted Absolute Error, Power System Stability, Power System Stabilizer.

INTRODUCTION

Power system stability is the ability of an electric grid to regain a state of operating synchronism after being subjected to a physical disturbance such as a fault or load change, ensuring that the system remains intact without widespread outages. It is critical, and time-dependent property based on maintaining balance between generation and load. Instability results from large disturbance such as faults, line tripping or small, continuous fluctuations that exceed the system's ability to maintain equilibrium, leading to issues like rotor angle swings, voltage collapse, or frequency decay according to Aibangbee (2025). Author Grigsby, (2017) in his studies concluded that, due to the increasing demand for electric power, existing transmission networks have become weak, leading to poor quality of unreliable supply. Furthermore, it requires huge amount of money to develop or strengthen the existing transmission network, and, in some cases, even securing the right-of-way for new lines can be challenging. The flow of reactive power is a major cause of voltage drop along the line. Power losses in the system are primarily due to reactive currents according to Wadhwa, (2018). The fixed voltage profile at any moment determines the maximum reactive power (vars) that can be transferred over the transmission lines according to Turan, (2019). Flexible Alternating Current transmission systems (FACTS) controllers are used to enhance the power transfer capability of the transmission systems. Under suitable control of power flow during and after system faults to maintain stability of the system. Power flow in a given line can be increased up to the thermal limit by injecting the required amount of current through the series line impedance. The increasing usage of FACTS devices for the enhancement of power system oscillations damping, proper synergy of FACTS controller and power system stability (PSS) becomes essential. In recent times, many researchers, such as Sahu, P.R. *et al*, (2022); Jolfaei, M.G. *et al*, (2016) have proposed various intelligent methods for improving and enhancing power system stability (PSS) under different fault disturbances using coordinated control of FACTS controllers, such as Thyristor controlled series compensator (TCSC), Static VAR compensator (SVC), or static synchronous series compensator (SSSC) designed in combination with other FACTS controllers, using Genetic algorithm (GA), In their studies, Khadanga, R. K. and Satapathy, J.K. (2015). investigates the time delay method for the coordinated SSSC and power system stabilizer (PSSs) controller using a hybrid particle swarm optimization and gravitational search algorithm (hPSO)-(GSA) technique. Also, Kamarposhti, M.A. *et al*, (2022) in their paper analyzed the coordinated structure of SSSC and PSS using the Ant Colony Optimization (ACO) techniques. Researchers Khampariya, P. *et al*, (2022) conducted investigation on the coordinated SSSC and PSS design using a hybrid technique. Similarly, Kar, M.K.*et al*, (2021) and Rout, B. *et al*, (2018), in their separate studies discussed simultaneous tuning of PSS and SSSC controllers using Modified sine cosine algorithm (MSCA). Also, researchers Bindumol, E.K. *et al, (*2022) [35], utilized particle swarm optimization (PSO) to tune SSSC and PSS controllers. Authors Sahu, P.R. *et al*, (2021), suggested a coordinated structure of PSS and SSSC controllers using modified whale optimization algorithm (M-WOA). The coordinated Static Compensator (STATCOM) and PSS design using Seeker optimization algorithm (SOA) was discussed by Afzalan, and Joorabian (2013). Similarly, modified whale optimization algorithm-nelder-mead (MWOA-NM) algorithm was proposed by Sahu, P.R. *et al*, (2022) to coordinately tune the PSS and SSSC parameters.

Fortes, *et al*, (2022), discussed the simultaneous tuning of static synchronous series compensator and Power oscillation damping (SSSC-POD) with PSS using the mayfly optimization technique (MOA). Over the years, various algorithms have been proposed for modeling damping controllers that were based on PSS and FACTS. These optimization techniques though effective, they have specific drawbacks regarding convergence speed, local optimum trapping, and computational burden in power system applications.

This article proposes the optimization and simulations of power system stability FACTS controllers with power system stabilizer-based time delays using combine grasshopper optimization algorithm (GOA) with a fuzzy proportional-integral-derivative (PID) coordinated controllers. The novelty of combining GOA with fuzzy-PID coordinated controller is to address the simultaneous tuning of the PSS and FACTS controller considering time-delays, reduce objective functions, provides better stability and enhance faster settling times. Simulations of GOA optimized controller are compared with GA, DE, and WOA optimized techniques using various loading conditions and disturbances to demonstrates its superiority both in single machine infinite bus (SMIB) and multi-machine power systems.

MATERIALS AND METHODS

The SMIB system was evaluated, as depicted in Figure 1 comprising of a synchronous generator that was linked to an infinite bus with the assistant of a transformer and an SSSC. The hydraulic turbine and governor (HTG) equipped in the generator signifies a non-linear hydraulic turbine model, a servomotor, and a proportional-integral-derivative (PID) governor system. Some other existing equipment within the generator includes the excitation system consisting of a DC exciter and a voltage regulator, without saturation function of the exciter and a PSS.

The transformer; the infinite bus and generator terminal voltages shown in Figure 1 were represented by V_B and V_T, while V_1 and V_2 are the bus voltages and, the output voltage of the SSSC converter. The DC voltage source is represented by V_{cnv} and V_{DC}; the line current represents I. The total real power flow in the transmission lines and that of a single line were each represented by P_L and P_{LL}, respectively.

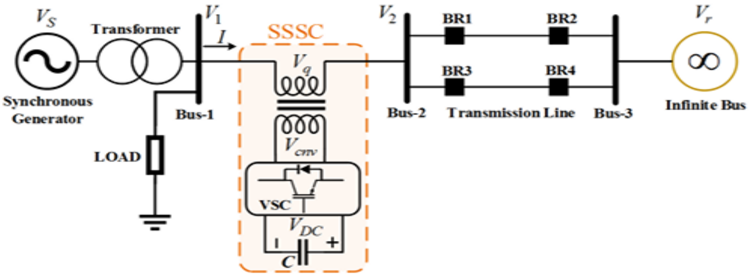

Figure 1: Circuit Diagram of Single Machine Infinite bus System with FACTS Controller

Static Synchronous Series Compensator (SSSC)

A static synchronous series compensator (SSSC) is a flexible AC transmission system (FACTS) device that enhances power system stability by injecting a controllable quadrature voltage in series with a transmission line, effectively acting as a controllable inductive or capacitive reactance. It improves small-signal stability, damps power oscillations, and increases transient stability limits through rapid response voltage source converter (VSC) technology. It consists of a VSC, a DC energy source or capacitor, and a coupling transformer. It functions include to: regulate line voltage; modifies the line reactance to control power flow as well as uses feedback signals to control the injected voltage, which helps to damp power system oscillations. The benefits of SSSC in stability studies are that it injects a sinusoidal voltage V_{Pq} in series with the line, which is kept in quadrature with the line current, I_L. This allows the SSSC to change the effective line impedance thereby, controlling active power flow and enhancing system stability. It can operate in multiple modes to improve system stability, with the constant reactance mode often providing better damping of inter-area oscillations and stability margins than constant voltage modes; as well as stability improvement in areas such as (i) small-signal stability especially with additional damping controllers can increases the damping of inter-area oscillations, and (ii) it assists in maintaining stability during large disturbances, such as faults, by manipulating the power transfer capabilities of the line.

In their study, (Elenilson *et al*, 2022) stated that, FACTS are represented by a voltage source converter (VSC) connected in series with the transmission line. This device varies the effective impedance of the line by injecting a voltage in phase with respect to the line current, thus allowing the exchange of active and reactive powers with the transmission system. According to (Elenilson, *et al*, 2022), Figures 2(a) and (b), shown the schematic diagram and equivalent circuit of the SSSC are shown, respectively.

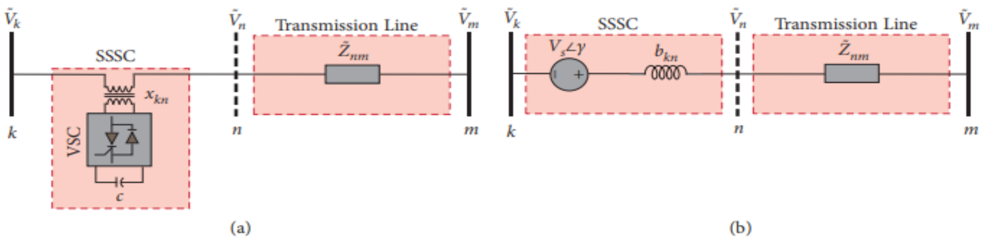

Figure 2: The SSSC FACTS and (b) Equivalent Circuit of the SSSC (Source: Elenilson *et al*, 2022)

In Figure 2(a), the SSSC is represented using a VSC in series with the transmission line. The VSC is connected to the system through a coupling transformer with a reactance x_{kn}, and by means of gate turn-off thyristors, it modulates a DC voltage coming from an external source. In Figure 2 (b), the phase angle δ of the voltage source V_s is represented by (1). Furthermore, $b_{kn} = -1/x_{kn}$ is the susceptance of the coupling transformer, and V_k and V_m are, respectively, the voltage phasors at buses k and m. Finally, V_n is the voltage phasor at the fictitious bus n, included in the system to perform simulations with the SSSC, and Z_{nm} is the impedance of the transmission line between buses n and m: (Elenilson *et al*, 2022)

δ = arctan V_p/V_q (1)

where $0 \leq \delta \leq 2\pi$, V_q and V_p are, respectively, the in-phase and quadrature components of the voltage source V_s.

Transmission Time Delays

Transmission time delay is the lag between the input signal and the system response. Time delay can be caused by factors like computational processing time, data transmission lags, inherent system characteristics. It causes significant adverse effects across network systems and power grid. The primary consequence is performance degradation, instability or even complete failure of the control system, where system become sluggish, unstable, or inaccurate. Thus, the proposes study is aimed to compensate for the time delay and mitigate the adverse effects of dead-time, ensuring smoother, and fast damping response settling time so as to maintain system reliability.

Adverse effects of time-delay on system performance are such that time-delays can significantly affect the performance of control systems. Minor delays in real time applications can cause discrepancies between the expected and actual outputs. This can be particularly detrimental in system that require precise timing and synchronization in system stability. Time delay can lead to oscillations, induce high-frequency oscillations in power networks, increased overshoot, or prolonged settling times, ultimately compromising the system stability and precision. If the time-delay is long enough, it can cause the entire control system to become unstable, leading to potential blackout and system failure in power grids. Consequently, managing time-delays is paramount in ensuring that control systems operate effectively and fulfill their intended functions.

Proposed Fuzzy Structured FACTS Controller with PSS

A fuzzy lead-lag coordinated with proportional integral device (F-PID) controller was designed for both PSS and FACTS devices optimization-based to minimize the impact of time delay signals. The design of the fuzzy logic controller (FLC) cascaded with proportional integral derivatives (PID) controller, referred to as fuzzy-PID (FPID) controller, was carried out at the Faculty of Engineering (Electronic Engineering Laboratories) using the triangular Membership Functions (MFs). The structure of the FPID controller is depicted in Figure 5, where ACE is the area control error taken as input to the FPID controller; K_1; K_2 are the input scaling factors and K_p; K_I; and K_D are the output scaling factors. Thus, the inputs and outputs scaling factors of the FPID controller was suitably selected to enhance the transient performance of the system. It is extensively used in Transmission lines because of its superior reliability, structural simplicity, and effective performance. The FLC has four components. (a) The fuzzifier which alters the value into fuzzy sets. (b) The fuzzy inference system that performs all the logical manipulations. (c) The rule base which contains the control rules and MFs. (d) The fuzzy inference system's output that is transformed into real value by the defuzzification technique as discussed by Fathy *et al*, (2020). The triangular MFs are commonly accepted in FLC strategies because of their real-time applications, economical nature, and improved performance according to Sahu *et al*, (2014).

The proposed fuzzy controller structure consists of seven triangular MFs, as depicted in Figure 6. According to Mohamed Barakat (2022); Sekhar *et al*, (2016); Mahto, *et al*, (2018) the authors emphasized in their studies that the fuzzy inputs are the ACE and the rate of change of Δ ACE derivative. The outputs were converted into seven linguistic variables Negative Large (NL), Negative Medium (NM) Negative Small (NS), Zero Error (ZE), Positive Small (PS), Positive Medium (PM), and Positive Large (PL).

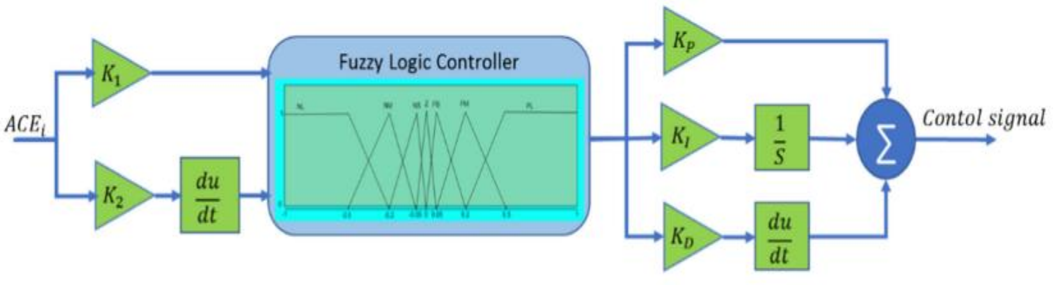

Figure 3: Structure of Fuzzy-PID Controller (Source: Mohamed Barakat (2022))

In order to obtained simplicity, enhanced computational efficiency, smaller amount of memory usage, and enhanced performance analysis, identical MFs with a similar range are used for both the inputs and the FLC design's output. The proposed rules which relate the inputs and outputs of the FLC is presented in Table 1. The fuzzy rules represent a significant function in the FLC performance. The designed optimum FPID controller, enable the gains/factors to be appropriately tuned. The dynamic response has minimum settling time, in seconds, with a trivial overshoot and undershoot, in hertz, when the system is subjected to adequate perturbation. In this study, a robust GOA technique is used to adjust the FPID controller to extract greater dynamic performance from the AGC-controlled FPID.

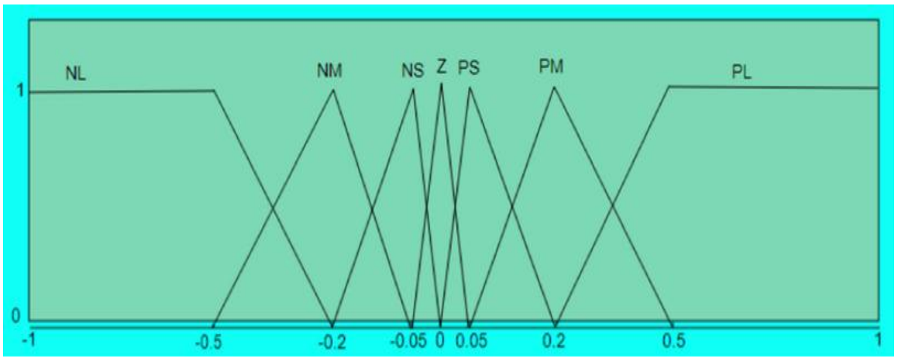

Figure 4: MFs of the FPID Controller for Error, Error Derivative, and the Output of FLC (source: Mohamed Barakat (2022))

Table 1: Rules Base for Error, Error Derivative, and FLC Output

Input 1 ACE	**ΔACE**						
	NL	**NM**	**NS**	**ZE**	**PS**	**PM**	**PL**
NB	ZE	ZE	NS	NM	PM	PM	PL
NM	ZE	ZE	ZE	NS	PS	PM	PL
NS	ZE	ZE	ZE	ZE	PS	PM	PL
ZE	NL	NM	NM	ZE	PS	PM	PL
PS	PL	NM	NM	ZE	ZE	ZE	ZE
PM	NL	NM	NM	PS	ZE	ZE	ZE
PB	NL	NM	NM	PM	PS	ZE	ZE

The SSSC injected voltage V_q is governed by the damping controller, which is based on the PSS and SSSC. This V_q is used for damping and hence can be considered the controller output while inputting the speed deviation (Δω). The SSSC controller injected voltage V_q is governed by the damping controller, which is based on the PSS and SSSC. This injected voltage V_q is used for damping and hence can be considered the controller output while inputting the speed deviation (Δω). The proposed controller comprised of two lead-lag components, as shown in Figure 3. A two-staged SSSC structure comprises of a gain block with gain T_{PS}, and a signal washout block serving as a high-pass filter shown is depicted in the figure, and a phase compensation block to provide appropriate phase-lead characteristics between input and output signals. The output of the PSS structure is shown in Figure 4. The Vs cumulate with the reference voltage of the excitation system, V_{ref}. Based on the washout function's perspective, the time constant value $T_{WS} = T_{Wp}$ lie somewhere between 1–20 s and is not critical. In the analysis, K_{PS} and T_{pp} are the controller gains, k_{1s}, k_{2s}, k_{3s} and k_{1p}, k_{2p}, k_{3p} are the scaling factors and time constants (T_{1s}, T_{2s}, T_{3s}, and T_{4s}) to be computed.

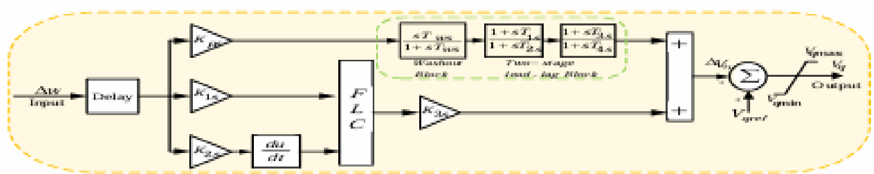

Figure 5: Proposed Fuzzy Lead-lag Structured SSSC Controller

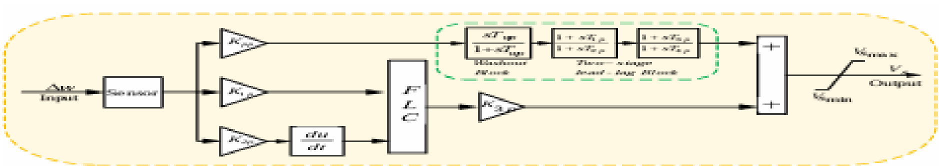

Figure 6: Proposed Fuzzy Lead-lag Structured Power System Stabilizer

In any control system, there is an unavoidable communication time delays in modern wide-area monitoring and control systems that is inherently present. A communication delay in a power grid is defined as the time between sending a signal from the source device to the receiving of the signal at the destination device. The SSSC devices are installed at locations that are far away from the generating units. The speed deviation of the generator is taken as an input signal to the proposed fuzzy lead-lag structured SSSC controller, as shown in Figure 3. Transmitting the speed deviation signal from the generator to the SSSC controller will take some time; thus, the time delay is included for the SSSC controller. Owing to the advancement in optical fiber communication, synchronous phasor measurement was performed by a wide-ranging measuring system that was then transmitted simultaneously to control centers. Thus, considering generator angle and speed deviation as remote signals, they were utilized for designing purposes. In the worst scenarios, a dedicated channel of communication not exceeding a delay of 50 ms during signal communication is recommended. So, the remedial solution is to take care of the time delays of this order during the designing of the controller. Considering improvement of the power system stability, the remote speed deviation signal is preferred over the local tie-line power and line current signals for damping controllers based on FACTS. Thus, a 15 ms sensor time constant and 50 ms time delayed signal transmission was each considered for PSSs and SSSC-based controllers, respectively.

Optimization Process

In this study, a pre-specified $T_{WS} = T_{WP}$ of 10s was used. The optimization process determined the time constants along with gains associated with the controller. As ΔV_q is zero during steady-state conditions, V_{qref} becomes constant. During dynamic conditions however, the modulation of the injected series voltage V_q is carried out by applying a certain algorithm in order to damp out the system oscillations. Due to slow operation of the power flow loop during the steady state, V_{qref} can be assumed to be constant. Thus, under dynamic conditions, the effective value of V_q can be formulated as

$$V_q = V_{qref} + \Delta V_{q1} \quad (2)$$

The system oscillation can be observed with the assistant of any one of the remote signals such as speed–deviation, tie-line power, or the deviation in the power angle. In the proposed study, the two objective functions that were considered are (*i*) An integral time absolute error (ITAE) of speed deviation for the SMIB power system and *(ii)* Speed signals corresponding to the inter-area and local oscillation modes. Both objective functions were expressed in equations (3) and (4)

For the single machine infinite bus power system:

Objective function value J = $\int_0^t |\Delta\omega| \,.\, t \,.\, dt$ (3)

And for power systems consisting of multiple machines:

Objective function value J = $\int_0^t (\sum|\Delta\omega_L| + \sum|\Delta\omega_I|\,).\, t \,.\, dt$ (4)

where t = time range of simulation, and $\Delta\omega$ = speed deviation. For the purpose of the objective function, the timed domain simulation of the power system model was performed for a specified time period using MATLAB/Simulink software. The range of the damping controller and PSS lie within the prescribed bounds. The system response in terms of settling time and overshoots improvement was achieved by minimizing the objective function. Thus, the optimization process is expressed from the design approach as expressed in (5),

Minimize objective function value J (5)

Subject to

$$K_{IS}^{min} \le K_{IS} \le K_{IS}^{max} \quad K_{IP}^{min} \le K_{IP} \le K_{IP}^{max}$$
$$K_{2S}^{min} \le K_{2S} \le K_{2S}^{max} \quad K_{2P}^{min} \le K_{2P} \le K_{2P}^{max}$$
$$K_{3S}^{min} \le K_{3S} \le K_{3S}^{max} \quad K_{3P}^{min} \le K_{3P} \le K_{3P}^{max}$$
$$K_{ps}^{min} \le K_{ps} \le K_{ps}^{max} \quad K_{pp}^{min} \le K_{pp} \le K_{pp}^{max}$$
$$T_{IS}^{min} \le T_{IS} \le T_{IS}^{max} \quad T_{IP}^{min} \le T_{IP} \le T_{IP}^{max} \quad (6)$$
$$T_{2S}^{min} \le T_{2S} \le T_{2S}^{max} \quad T_{2P}^{min} \le T_{2P} \le T_{2P}^{max}$$
$$T_{3S}^{min} \le T_{3S} \le T_{3S}^{max} \quad T_{3P}^{min} \le T_{3P} \le T_{3P}^{max}$$
$$T_{4s}^{min} \le T_{4s} \le T_{4s}^{max} \quad T_{4p}^{min} \le T_{4p} \le T_{4p}^{max}$$

where the min. and max. superscripts represent the lower and upper values of the corresponding parameter. The minimum and maximum values of the parameters were set at 0.0 and 2.0, respectively.

In order to optimized for a single machine infinite bus system consisting of one damping controller and one power system stabilizer, two gains, eight-time constant parameters, and six scaling factors were needed. Similarly, damping controllers equivalent to the number of generators, optimization was carried out on all the parameters for a power system composed of multiple machines such as multiple power system stabilizer (PSSs).

Grasshopper Optimization Algorithm (GOA) Technique

Grasshopper optimization algorithm (GOA) is a swarm-based metaheuristic inspired by the foraging behavior of grasshoppers, balancing global exploration and local exploitation through dynamic adjustments in repulsion and attraction forces. In their studies, Sahu, P.R. *et al*, (2022); and Saremi, *et al*, (2017) demonstrated that the Grasshopper Optimization Algorithm (GOA) benefits from high exploration while exhibiting very fast convergence speed. Exploration and exploitation balance smoothly with the unique adaptive mechanism in this algorithm. These features possibly enable the GOA algorithm to deal with greater exploration of search space and outperform other methods. Furthermore, computational complexity is superior to that of many techniques, such as GA, DE, and WOA.

The mathematical model designed in this paper for the swarming behavior of grasshoppers is presented in (7),

$$X_i = S_i + F_i + W_i \quad (7)$$

where X_i , S_i , F_i and W_i denotes the *i*-th grasshopper's position; social interaction; the n-th grasshopper's gravitational force, and wind speed factor respectively. The above circumstances can be constructed as

$$X_i = r_1 I_1 + r_2 F_l + r_3 W_i. \quad (7b)$$

where r_1, r_2, and r_3 are randomized values selected between [0,1].

$$S_i = \sum_{\substack{l=1 \\ l \ne k}}^{N} s(d_{kl}).\hat{d}_{kl} \quad (8)$$

where d_{kl} signifies the distance of k-th from l-th grasshopper. It is calculated as $d_{kl} = |X_l - X_k|$ and s represent the force that describes the potency of social interaction forces and $\hat{d}_{kl} = \frac{|X_l - X_k|}{d_{kl}}$ is a unit vector from k-th grasshopper to l-th grasshopper. The social interaction forces (S_i), governs the attraction or repulsion between agents based on a comfort zone, determined by a function calculated as:

$$s\,(r) = \alpha e{-}(r/l) - e^{-r} \quad (9)$$

where α is the intensity of attraction, and l represents attractive length of scale. This function describes the effect on grasshopper communal interaction according to Afzalan, and Joorabian (2013). The function's' segregates the space between two grasshoppers into attraction, repulsion, and comfort zones. However, this function returns zero value if the separation between two grasshoppers is more than 10. Hence, with larger separation, this function fails to apply forces between two grasshoppers. This paper mapped the separation between the grasshoppers to a value between 1 to 4. From equation (7), the F component is calculated as:

$$F_i = -g\hat{e}_g \quad (10)$$

Where g is the gravitational constant, and e_g is the unity vector directed towards the earth's center. The component W in equation (7) is calculated as $W_i = u\hat{e}_w$ (11)

where u is the drift constant and ew is the unity vector in the wind direction. By replacing equation (8), (10), and (11) in equation (7), solving the grasshopper swarming behavior can be represented as in (12),

$$X_i = \sum_{\substack{l=1 \\ l \neq k}}^{N} s(|X_l - X_k|)\frac{X_l - X_k}{d_{kl}} - g\hat{e}_g + u\hat{e}_w \quad (12)$$

where N is the number of grasshoppers.

A modified form of equation (11) is considered to resolve the optimization problems, as in (13)

$$X_i^d = c\left(\sum_{\substack{l=1 \\ l\neq k}}^{N} c\frac{ub_d - lb_d}{2} S(|X_l - X_k|).\frac{|X_l - X_k|}{d_{kl}}\right) + T_d \quad (13)$$

where ub_d and lb_d represent upper and lower bounds, in the D-th dimension. The T_d is the target value, the term S represents social interaction, and c is a decreasing constant that reduces the attraction, repulsion, and comfort zones.

Based on exploration, exploitation was used to locate food in potential local locations in order to obtain the best global value. when the number of iterations increases, c has a significant impact on the grasshopper's behavior. while the inner c reduces grasshopper attraction or repulsion forces, the outside c reduces the search space around the target maximum. In order to maintain the proper balance between exploration and exploitation, the value of c should decrease relative to the number of iterations. This phenomenon encourages the algorithm towards exploitation as the number of iterations increases. In proportion to iteration counts, the decreasing coefficient c diminishes the size of the comfort zone, as in equation (14)

$$C = C_{max} - I\ \frac{C_{max} - C_{min}}{t_{max}} \quad (14)$$

where C_{max} and C_{min} represent the maximum and minimum values, I is the current iteration, while t is the maximum number of iterations. The parameter C decreases linearly from 1 and 0.00001over the course of iterations, reducing the size of repulsion/attraction zones.

RESULTS AND DISCUSSION

The Sim Power Systems (SPS) toolbox was used extensively for the calculations and design of the damping controller using the SIMULINK environment with the MATLAB-based design tool SPS.

Power equipment such as transformers, transmission lines, power electronics, and machines models, are all present in its libraries. Three-phase machines load flow and initialization were performed with the help of the Power GUI block. Thus, the analysis of the developed models was carried out by the graphical user interface (GUI) tools embedded in it.

Single Machine Infinite Bus (SMIB) Power System

The power system model of SMIB designed and simulated in MATLAB consists of a generating unit in connection with a double-circuited parallel line transmission line as shown in Figure 7. It is connected between a step-up transformer and an SSSC. The GOA algorithm was employed using an m file for tuning the proposed controller. Simulation of the entire model was conducted along with simultaneous calculation of the objective function owing to the occurrence of any disturbance in the system using the MATLAB R2016a environment. The controller parameters were obtained by minimizing the fitness values of equation (3), whose optimization was conducted using the GOA algorithm. Table 2 depicts the optimized parameters. The dominance of the GOA technique was validated by comparing of the Integral of time-weight absolute error (ITAE) values of GA, DE algorithm, and WOA techniques as shown in Table 3. In this proposed simulation analysis, different parameters were initialized for the applications of GOA, GA, DE, and WOA. Maximum number of generation and population size are the common control parameters of the algorithms. In this paper, comparison between optimization techniques was carried out by considering the search agents of 30 and total iterations of 500. The selection of various parameter values for the GOA algorithm were carefully made for implementation and efficient performance.

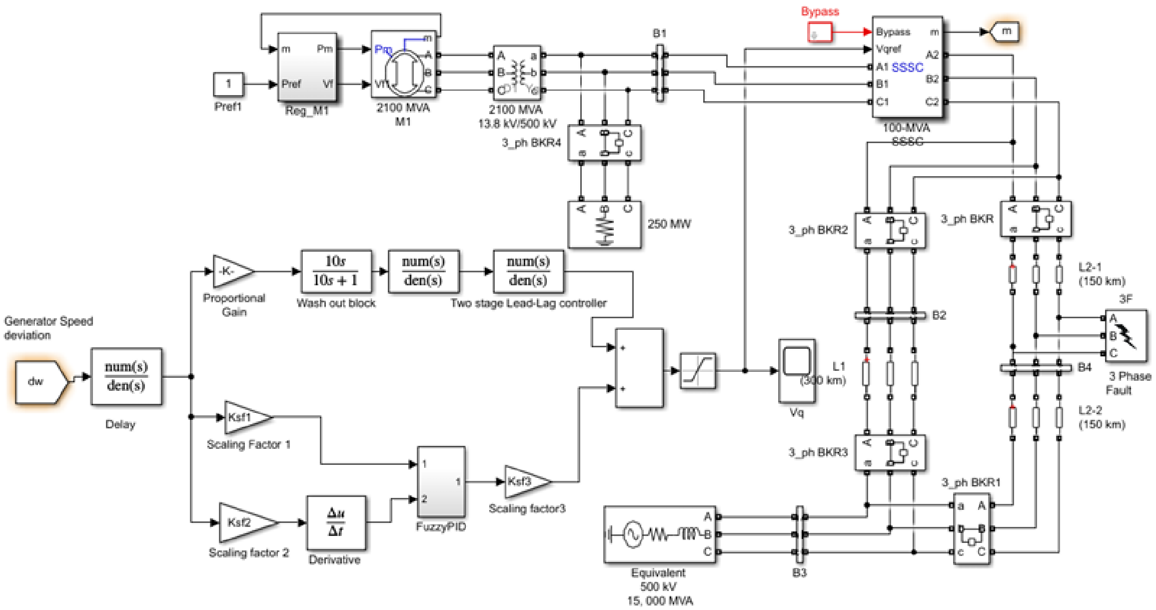

Figure 7: Proposed SMIB System in MATLAB/SIMULINK

Integral of time-weighted absolute error (ITAE) is a performance criterion used in power system engineering to optimize control systems such as PID controllers. In power system stabilizers (PSS) and FACTS devices, its acts as an objective function in simulations to tune controller gains like $(k_{p,}k_{\ i}\,k_d)$ to minimize errors overtime. Its role in power system stability include:

i. Optimal Tuning: The studies minimizing controller gains to minimize the ITAE objective function, it provides the lowest settling time compared to others; It helps find the best PID parameters that minimize both overshoot and settling time.

ii. Damping Oscillations: It is widely used to tune controllers to minimize low frequency inter-area oscillations; better damping and faster settling times compared to others controllers.

iii. Disturbance Rejection: It provides superior performance in ensuring that the 3-phase system quickly return to equilibrium after a disturbance.

iv. ITAE links overshoot and settling time by allowing a specific, well-damped, and relative quick oscillation that minimizes ITAE favoring a faster total response time over the smallest possible peak overshoot.

v. Settling Time Reduction: ITAE act as a strong driver for shortening settling time in reaching the set point quickly.

ITAE is a design criterion used to find the minimum possible settling time for a given system, often resulting in shorter settling times than traditional tuning method. Thus, GOA controller minimized the ITAE objective functions and provide faster settling time and lowest overshoot compared to DE, GA, and WOA. A more robust and fast-acting control system can be achieved by minimizing the ITAE values, thus enhancing the overall transient stability of the grid.

Table 2: GOA Optimized Proposed SSSC and PSS Parameters on SMIB System

Optimization Techniques	Parameters	K_{Pi}	T_{1i}	T_{2i}	T_{3i}	T_{4i}	K_{1i}	K_{2i}	K_{3i}
DE	SSSC Controller	21.92	0.2863	0.3348	1.2381	1.1442	1.714	1.861	1.9604
	PSS	2.985	1.8547	1.4521	1.4704	0.1299	1.7111	1.5652	1.0243
GA	SSSC Controller	89.35	0.2609	1.7593	1.7988	0.0797	0.9997	0.5602	0.6101
	PSS	67.39	0.4636	0.2424	1.094	1.8826	1.0157	0.2932	1.3673
WOA	SSSC Controller	65.27	1.5686	0.6974	0.7433	1.3132	0.5690	1.8089	0.0203
	PSS	15.68	1.0051	0.9367	0.4572	0.0042	0.8746	1.8253	0.7999
GOA	SSSC Controller	77.72	2.9233	1.7239	1.9148	3.1756	3.3627	1.3942	1.6512
	PSS	19.21	0.0576	1.3758	4.1737	1.7247	1.3127	2.1992	3.3943

Table 3: ITAE Values for Proposed GOA Optimized Techniques with GA, DE, and WOA

Case studies	DE	GA	WOA	GOA
Case 1 (x10^{-4})	9.304	9.395	9.593	8.026
Case 2 (x10^{-4})	3.795	3.094	2.328	1.982
Case 3 (x10^{-4})	3.415	3.218	2.903	2.104

Three different case studies were considered for evaluations as follows:

(i) Normal loading,

(ii) Light loading, and

(iii) Heavy Loading conditions.

Case study 1: Normal Loading Condition

The performance of the proposed controller was demonstrated at P_e = 0.85 pu, and δ_0 =52.3deg. These are the nominal loading conditions in terms of the occurrence of a severe disturbance in the system. At the mid-section of the transmission line linking bus-2 and bus-3 at time t =1s, a 3-cycles, 3-phase fault was imposed. The system returns to its original state after it was cleared. The system's various damping oscillations responses were indicated in Figures 10–13. These include speed deviation in pu, tie-line power P_L in MW, power angle δ in degree, and SSSC injected voltage V_q. From the different damping oscillations responses, it was cleared that the GOA-optimized proposed controller provides faster and improved dynamic response when compared with GA, DE algorithm, and WOA optimized controllers.

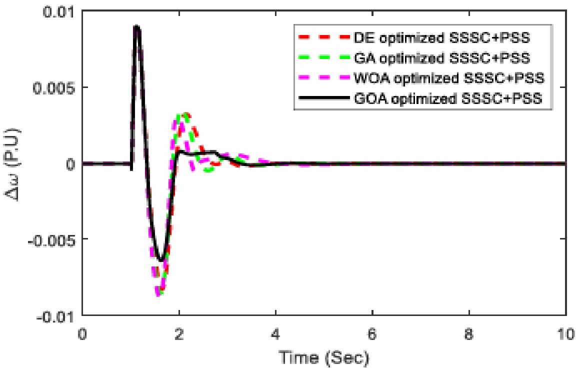

Figure 8: Normal Loading Speed Deviation

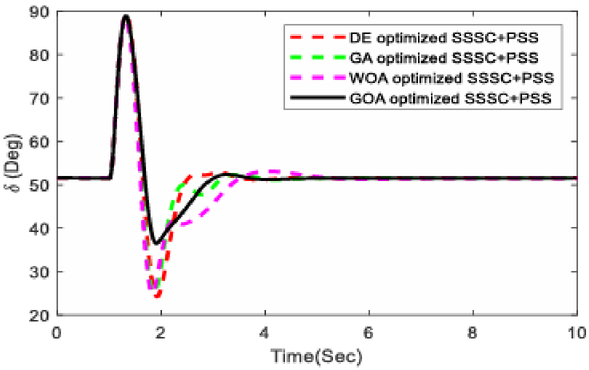

Figure 9: Power Angle Response

It can be observed that GOA-optimized controller offers faster and improved dynamin response in terms of minimal overshoot/undershoot and settling times; has better low-frequency oscillation damping capabilities and can easily stabilize the device by adjusting the SSSC-injected voltage compare with WOA, DE, and GA-optimized controllers as presented in Figures 10 to13. The propose controller increases the restriction on power system stability and capacity.

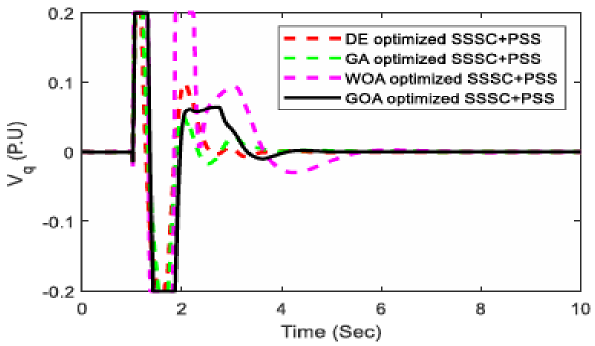

Figure 10: SSSC Injected Voltage

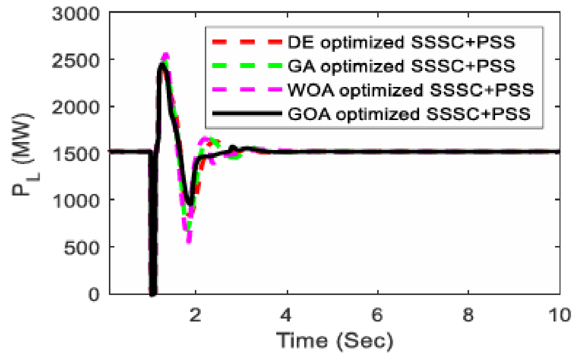

Figure 11: Normal Loading Tie-line Power

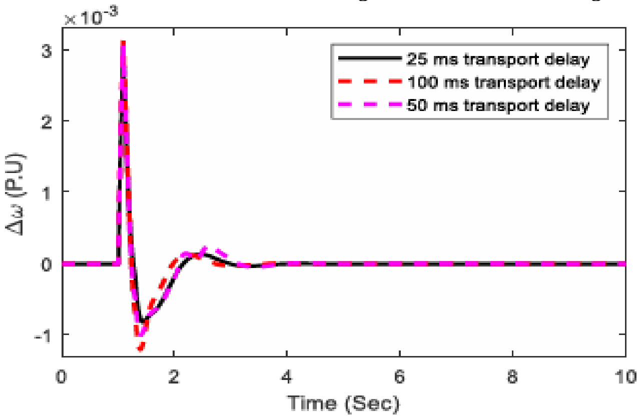

Figure 12: Transmission Line Delays Due to Speed Deviation

Figure 14 display various transmission delays considering speed deviation. It is shown from the figure that the GOA controller damping response with a transport delay of 25ms speed deviation, it indicates faster settling times; ensure stability for normal loading conditions.

Case Study 2: Light Loading Condition

The superiority of the proposed controller, was tested by changing the generator's loading state to light loading of P_e= 0.5 p.u. and δ_0 = 33.23deg. A 5-cycle 3-phase fault arises, at the midpoint of the transmission line, followed by load removal at t =1.0s at bus-1. The system's damping oscillations responses illustrates the quality of the propose GOA controller were shown in Figures 15 to 17 for changes in working conditions and types of disturbance.

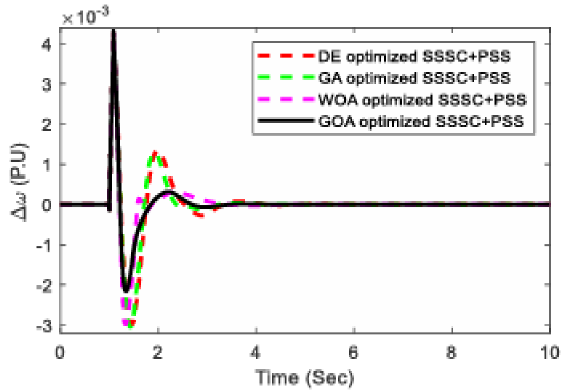

Figure 13: Light Load Speed Deviation Response

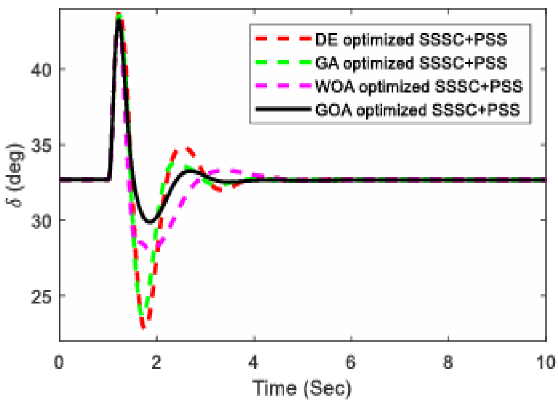

Figure 14: Light Load Power Angle Damping Response

when compared with GA, DE algorithm, and WOA controllers, the propose GOA technique delivers improved transient responses. The GOA-optimized coordinated design of the PSS and SSSC controller shown to have substantially suppresses the rotor angle swing; provides faster and better damping characteristics for electromechanical oscillation modes.

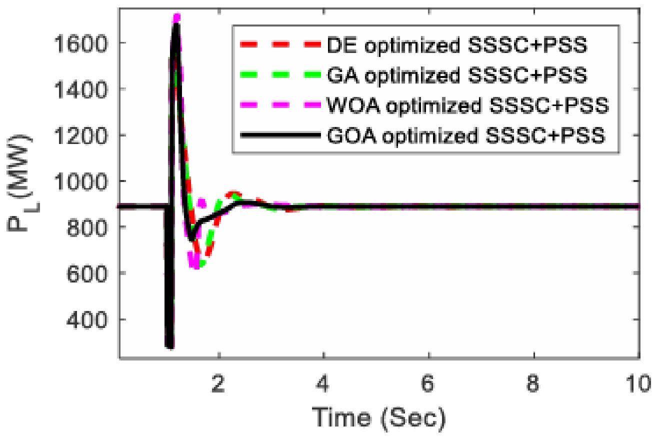

Figure 15: Tie-line Power

Case Study 3: Heavy Loading Condition

The robustness of this controller was carried out in this condition at P_e =1.0 pu and δ_0 = 60.73deg). The load was disconnected near bus 1 at t =1.0s for 300ms. The speed deviation response under heavy loading conditions is shown in Figure 18. The effectiveness of the GOA optimized proposed controller compared with GA, DE algorithm, and WOA optimized controller provides more reliable performance. Results shows that system stability was retained, and power system oscillations with the proposed controllers were effectively damped out. The ITAE values for the three loading conditions were plotted in Figure 19 to demonstrate the enhancement by the proposed GOA technique.

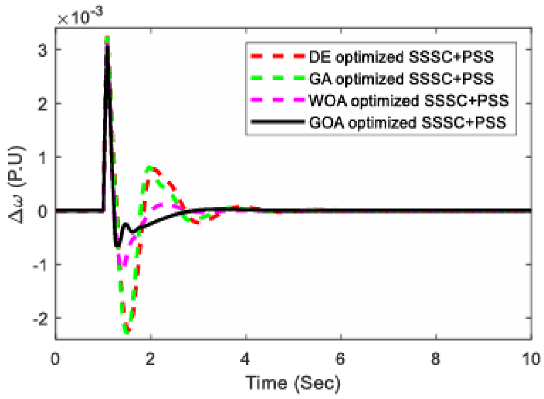

Figure 16: Heavy Loading Speed Deviation Response

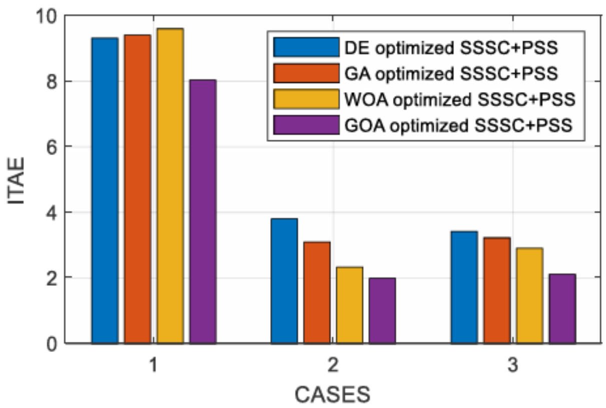

Figure 17: Comparisons of ITAE Values Proposed GOA with DE, GA, and WOA for SMIB System

Table 4 presents the performance of DE/GA/WOA/GOA optimized controllers based on SMIB system's transient response parameters. These indices are used as objective functions to evaluate and compare the controller's performances in seconds.

Table 4: Transient Response Parameters Optimized with DE/GA/WOA/GOA Algorithms

Studied Algorithms	**Speed Deviation Case study 1**			**Speed Deviation Case study 2**			**Speed Deviation Case study 3**		
	undershoot ($x10^{-3}$)	**Setling Time**	**ITAE ($x\ 10^{-3}$)**	**undershoot ($x10^{-3}$)**	**Setling Time**	**ITAE ($x\ 10^{-3}$)**	**undershoot ($x10^{-3}$)**	**Setling Time**	**ITAE ($x\ 10^{-3}$)**
DE	-8.45	3.41	9.26	-2.93	3.67	3.75	-2.19	4.00	3.37
GA	-7.6	3.37	9.35	-2.99	3.39	3.05	-2.23	3.35	2.18
WOA	-8.55	3.60	9.55	-2.93	3.08	2.28	-1.05	3.34	2.905
GOA	-6.29	3.27	7.97	-2.10	2.69	1.93	-61	2.65	2.06

Multi-Machine Power System

Power system circuit diagram involving multiple machines and tie lines is shown in Figure 20. The SSSC controller is placed between bus 5 and bus 6.

Two case studies were selected for evaluations purposes as follows:

(i) Three-Phase Fault Disturbance
(ii) Small Disturbance

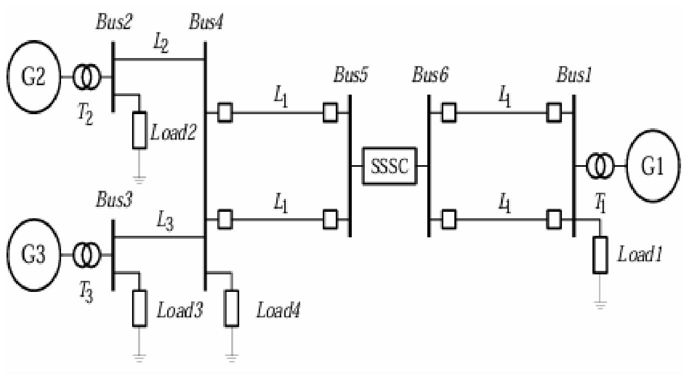

Figure 18: Multi-machine System

Case Study 1: Three-Phase Fault Disturbance
A 3-phase self-clearing fault was initiated at the line joining bus1 and bus 6 at t = 1s. The fault duration was taken as a 3-cycle. At bus 6, the system gains back to its original state after clearing the fault. Figures 21and 22 shown the response of the system.

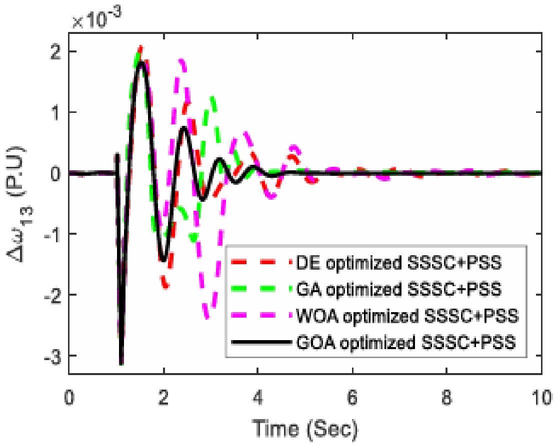

Figure 19: Inter-area mode of Oscillations

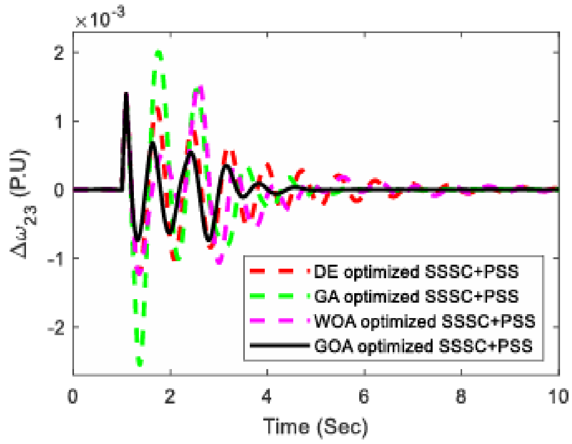

Figure 20: Local-area mode of Oscillations

From these figures, the local mode and inter-area modes of damping oscillations response were observed to be greatly oscillatory with GA, DE, and WOA controllers. By modulating the SSSC injected voltage and stabilization of the PSSs signals, the proposed GOA controllers suppress the damping oscillations responses quickly and offers improved stability of the power system significantly. The effectiveness of the proposed coordinated design is validated by varying the transport delay signals. A time delay of 50ms was analyzed at start for the signal transmission. Figures 23 (a) and (b) demonstrates the damping responses of the system. It shows that the variation in time delay have a remarkable improvement and shorter settling times of 25ms on the propose GOA controller performance, as compared to the 100ms transport delay with other controllers.

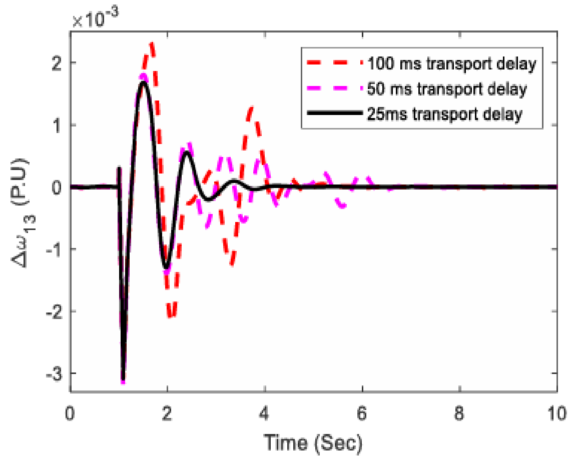

(a) Inter-area Damping Oscillations

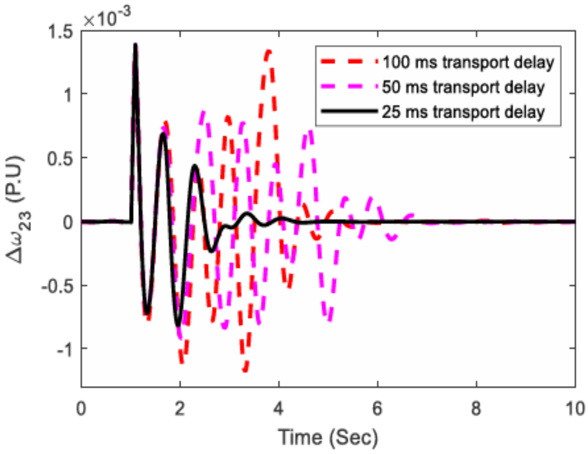

(b) local-area Damping Oscillations

Figure 21: Transmission Time Delay

Case Study 2: Small Disturbance

The system was evaluated with a small disturbance to ensure the complete assessment of the proposed controller's performance. The load was detached at bus 4 and simulated from t =1.0s for a duration of 100ms. Figures 24 and 25 illustrate the system damping response for the case studied. The figures illustrate the efficacy of PSS and SSSC in the damping of low-frequency oscillations. It revealed that the GOA-optimized coordinated design responses damp out quickly, maintained stable and ensures stability in all loading conditions as compared to other controllers under considerations. The robustness and efficient damping quality of the proposed controller under this condition is clearly justified.

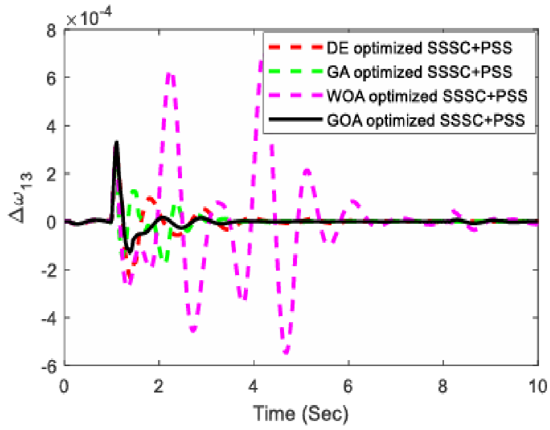

Figure 22: Inter-area Damping Oscillations Response

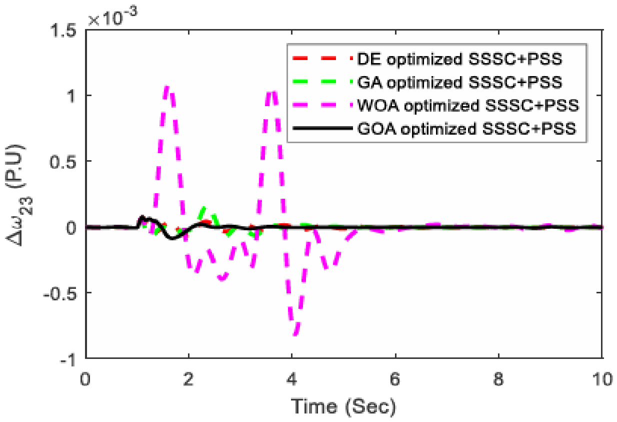

Figure 23: Local-area Damping Oscillations Response

The proposed GOA-optimized controller significantly performs better than the WOA, DE, and GA-optimized controllers in terms of dampening power system oscillations and reduce settling time. The ITAE values for the two case studies of the multi-machine system were presented in a bar chart as shown in Figure 26 to better illustrate the improvement by the proposed method. The proposed technique offers enhanced damping performance against oscillations and improved stability margins under varying load conditions, accounts for potential instabilities from time-delays, and convergence to an optimum global value.

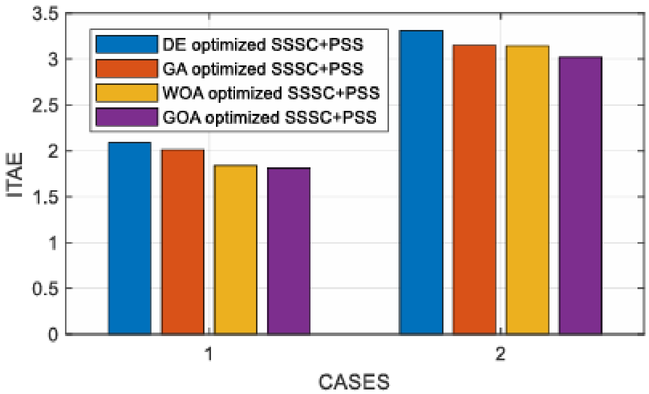

Figure 24: Comparisons of ITAE Values for Propose GOA with DE, GA, and WOA

Table 5 shows the optimum parameters of the proposed controller for multi-machine systems.

Table 5: GOA Proposed SSSC and PSS Optimized Parameters

Optimization Techniques	Parameters	K_{Pi}	T_{1i}	T_{2i}	T_{3i}	T_{4i}	K_{1i}	K_{2i}	K_{3i}
DE	SSSC Controller	11.40	0.1291	0.0156	0.1261	0.0783	0.0284	0.1024	0.0460
	PSS 1	1.59	0.0485	0.0373	0.0454	0.0176	0.1301	0.0630	0.1117
	PSS 2	7.015	0.0142	0.1112	0.0940	0.0329	0.1025	0.1713	0.1753
	PSS 3	2.99	0.0491	0.1167	0.1310	0.0886	0.0486	0.1894	0.0251
GA	SSSC Controller	148.30	1.3754	0.5408	0.7549	1.7236	3.2910	0.5985	0.0181
	PSS 1	115.06	1.7811	1.6894	0.2465	1.0716	1.6734	3.7250	0.7136
	PSS 2	5.455	1.7966	1.6361	1.3506	0.2686	0.3820	2.0262	1.3585
	PSS 3	156.31	0.2102	1.5964	1.4979	1.3699	0.9229	1.6267	1.7357
WOA	SSSC Controller	18.66	0.1416	0.0732	0.3436	0.2197	0.0945	0.3551	0.2213
	PSS 1	17.98	0.1220	0.3326	0.1265	0.1570	0.3435	0.2847	0.1089
	PSS 2	5.065	0.0326	0.1801	0.2329	0.1077	0.2467	0.3471	0.0631
	PSS 3	12.045	0.0612	0.0339	0.0239	0.2344	0.2939	0.2085	0.2349
GOA	SSSC Controller	19.395	0.2693	0.1574	0.2645	0.3332	0.2964	0.2240	0.0382

Optimization Techniques	Parameters	K_{Pi}	T_{1i}	T_{2i}	T_{3i}	T_{4i}	K_{1i}	K_{2i}	K_{3i}
	PSS 1	7.74	0.1340	0.3025	0.1269	0.0169	0.1897	0.3469	0.0033
	PSS 2	19.235	0.2735	1.1766	0.3186	0.0298	0.1170	0.3694	0.0614
	PSS 3	8.615	0.0503	0.1324	0.0980	0.1956	0.2867	0.3525	0.0333

Table 6 illustrates that GOA methods which take into consideration, the multiple instances had the lowest ITAE values when compared with DE, GA, and WOA methods.

Table 6: ITAE Values Assessment for Multi-machine System

Case Studies	DE	GA	WOA	GOA
Case 1 (x 10^{-4})	2.084	2.007	1.832	1.806
Case 2 (x 10^{-4})	3.306	3.145	3.137	3.016

The findings revealed that GOA optimized controller outperfoms both the DE, WOA and GA in damping oscillations response in control optimization problems such that:

i. Overshoot: GOA exhibits superior performance in minimizing overshoot, meaning it brings systems to steady-state with fewer dramatic peaks.
ii. Settling Times: GOA demonstrates faster convergence and settling times in transient response studies. While DE, WOA, and GA are often quite slow, GOA frequently shows superior speed in reaching stability, which means, it shows lower ITAE values.
iii. Comparison: While GA, DE, and WOA are both nature-inspired and modern, GOA often proves more robust in damping oscillations because its "comfort zone" parameter linearly decreases, allowing it to transition more efficiently from exploration to exploitation, reduces excessive oscillation in the final convergence phase.
iv. Stability: GOA tuned controllers shows enhanced transient response, maintained stability, and provides better convergence characteristics than WOA, DE, and GA controllers under various loading conditions
v. The proposed GOA optimized controller reduced the objective function values by 16.29% better than WOA (14.53%), GA (14.53%), and DE (13.69%), in the SMIB system and 1.43%, 9.95%, and 13.33%, for the multi-machine systems.

CONCLUSION

This article proposes the optimization and simulations of power system stability FACTS controllers with coordinated power system stabilizer-based time delays using grasshopper optimization algorithm (GOA). Evaluation performances of damping controller based on PSS and SSSC was conducted to analyzed the single machine infinite bus (SMIB) and the multi-machine system. The proposes GOA technique was utilized to achieve proper tuning of the controller parameters optimally and coordinately. A fuzzy lead-lag cascaded with proportional integral device (F-PID) controller was designed for both PSS and FACTS devices optimization-based to minimize the impact of time delayed signals was analyzed and the proposes rules which relate the inputs and outputs of the FLC was presented. For the purpose of the objective function, the timed domain simulation of the power system model was performed for a specified time period using MATLAB/Simulink software. The effectiveness of the implemented coordinated algorithm was tested through the simulation results obtained at various load conditions and disturbances. The technique offers enhanced damping performance against oscillations and improved stability margins, accounting for potential instabilities from time-delays. The proposes GOA technique transient response parameters was analyzed to have the lowest values in terms of ITAE, undershoot, and settling times in the SMIB system as well as for a multi-machine system and presented. The effectiveness of the GOA was validated with various load conditions and disturbances. It also revealed that, the GOA controller performed excellently, effective, superior, robust enough to manage faults and variations in operating conditions compared with GA, DE, and WOA controllers respectively.

REFERENCES

Afzalan, E; Joorabian, M. Analysis of the simultaneous coordinated design of STATCOM-based damping stabilizers and PSS in a multi-machine power system using the seeker optimization algorithm. Int. J. Electr. Power Energy Syst. 2013, 53, 1003–1017. [CrossRef]

Aibangbee (2025) “Power System Stability Improvement using Flexible A.C Transmission System (FACTS) Controllers” Journal of Engineering Research Innovation and Scientific Development 3 (2), (2025), 42-45 https://doi.org/10.61448/jerisd32258

Bastos-Filho, C.J.; Chaves, D.A.; Silva, F.S.; Pereira, H.A.; Martins-Filho, J.F. Wavelength assignment for physical-layer-impaired optical networks using evolutionary computation. J. Opt. Commun. Netw. 2011, 3, 178–188. [CrossRef]

Bindumol, E.K.; Mini, V. Chandran, N. Coordinated Control of PSS and SSSC using PSO to Improve Power System Stability. In Emerging Technologies for Sustainability; CRC Press: Boca Raton, FL, USA, 2020; pp. 293–302.

Elenilson V. Fortes, Luı´s Fabiano Barone Martins, Marcus V. S. Costa , Luis Carvalho , Leonardo H. Macedo , and Rube´n Romero (2022)” Mayfly Optimization Algorithm Applied to the Design of PSS and SSSC-POD Controllers for Damping Low-Frequency Oscillations in Power Systems” International Transactions on Electrical Energy Systems Volume 2022, https://doi.org/10.1155/2022/5612334

Fathy A, Kassem AM, Abdelaziz AY (2020) Optimal design of fuzzy PID controller for deregulated LFC of multi-area power system via mine blast algorithm. Neural Computing and Application 32(9):4531–4551. https://doi.org/10.1007/s00521-018-3720-x

Fortes, E.V.; Martins, L.F.; Costa, M.V.; Carvalho, L.; Macedo, L.H.; Romero, R. Mayfly Optimization Algorithm Applied to the Design of PSS and SSSC-POD Controllers for Damping Low-Frequency Oscillations in Power Systems. Int. Trans. Electr. Energy Syst. 2022, 2022, 5612334. [CrossRef]

Grigsby L.L(2017) Power System Electric Power Engineering Handbook 2nd Edition Publisher Taylor & Francis Group, LLC.

Jolfaei, M.G.; Sharaf, A.M.; Shariatmadar, S.M.; Poudeh, M.B. A hybrid PSS–SSSC GA-stabilization scheme for damping power system small signal oscillations. Electr. Power Energy Syst. 2016, 75, 337–344. [CrossRef]

Kamarposhti, M.A.; Colak, I.; Iwendi, C.; Band, S.S.; Ibeke, E. Optimal coordination of PSS and SSSC controllers in power system using ant colony optimization algorithm. J. Circuits Syst. Comput. 2022, 31, 2250060. [CrossRef]

Kar, M.K.; Kumar, S.; Singh, A.K.; Panigrahi, S. A modified sine cosine algorithm with ensemble search agent updating schemes for small signal stability analysis. Int. Trans. Electr. Energy Syst. 2021, 31, e13058. [CrossRef]

Khadanga, R.K.; Satapathy, J.K. Time delay approach for PSS and SSSC based coordinated controller design using hybrid PSO–GSA algorithm. Electr. Power Energy Syst. 2015, 71, 262–273. [CrossRef]

Khampariya, P.; Panda, S; Alharbi, H; Abdelaziz, A.Y.; Ghoneim, S.S. Coordinated Design of Type-2 Fuzzy Lead–Lag-Structured SSSCs and PSSs for Power System Stability Improvement. Sustainability 2022, 14, 6656. [CrossRef]

Khuntia, S.R.; Panda, S. ANFIS approach for SSSC controller design for the improvement of transient stability performance. Math. Comput. Model. 2013, 57, 289–300. [CrossRef]

Mahto T, Malik H, Saad Bin Arif M (2018) Load frequency control of a solar-diesel based isolated hybrid power system by fractional order control using partial swarm optimization. J Intell Fuzzy Syst 35(5):5055–5061

Mohamed Barakat (2022) Optimal design of fuzzy-PID controller for automatic generation control of multi-source interconnected power system Neural Computing and Applications (2022) 34:18859–18880 https://doi.org/10.1007/s00521-022-07470-4

Panda, S. Multi-objective evolutionary algorithm for SSSC-based controller design. Electr. Power Syst. Res. 2009, 79, 937–944. [CrossRef]

Panda,S.; Swain, S.C.; Rautray, P.K.; Malik, R.K.; Panda, G. Design and analysis of SSSC based supplementary damping controller. Simul. Model Pr. Theory 2010, 18, 1199–1213. [CrossRef]

Rout, B;Pati, B.B; Panda, S. Modified SCA algorithm for SSSC damping Controller design in Power System. ECTI Trans. Electr. Eng. Electron. Commun. 2018, 16, 46–63. [CrossRef]

Sahu BK, Pati S, Mohanty PK, Panda S (2015) Teaching–learning based optimization algorithm based fuzzy-PID controller for automatic generation control of multi-area power system. Appl Soft Computing 27:240–249

Sahu RK,Panda S, Yegireddy NK(2014) A novel hybrid DEPS optimized fuzzy PI/PID controller for load frequency control of multi-area interconnected power systems. J Process Control 24(10):1596–1608

Sahu, P.R.; Hota, P.K.; Panda, S. Modified whale optimization algorithm for coordinated design of fuzzy lead-lag structure-based SSSC controller and power system stabilizer. Int. Trans. Electr. Energy Syst. 2019, 29, e2797. [CrossRef]

Sahu, P.R.; Hota, P.K.; Panda, S.; Lenka, R.K.; Padmanaban, S.; Blaabjerg, F. Coordinated Design of FACTS Controller with PSS for Stability Enhancement Using a Novel Hybrid Whale Optimization Algorithm–Nelder Mead Approach. Electr. Power Compon. Syst. 2022, 1–6. [CrossRef]

Sahu, P.R.; Lenka, R.K.; Khadanga, R.K.; Hota, P.K.; Panda, S.; Ustun, T.S. Power System Stability Improvement of FACTS Controller and PSS Design: Sustainability 2022, 14, 14649. https://doi.org/10.3390/ su142114649.

Saremi, S.; Mirjalili, S.; Lewis, A. Grasshopper optimization algorithm: Theory and application. Adv. Eng. Softw. 2017, 105, 30–47. [CrossRef]

Sekhar GTC, Sahu RK, Baliarsingh AK, Panda S (2016) Load frequency control of power system under deregulated environment using optimal firefly algorithm. Int J Electr Power Energy Syst 74:195–211

Turan. (2019) Electrical power transmission system engineering: analysis and design. Second Edition. Taylor & Francis Group, LLC

Wadhwa C.L. (2018) Electrical power systems, New Academic science limited

Woo Z-W, Chung H-Y, Lin J-J (2000) A PID type fuzzy controller with self-tuning scaling factors. Fuzzy Sets Syst 115(2):321–326

\